



Cooperating minimalist nanovaccine with PD-1 blockade for effective and feasible cancer immunotherapy



Mingxia Jiang^a, Liping Zhao^a, Xiaoming Cui^a, Xinghan Wu^a, Yuhan Zhang^a, Xiuwen Guan^{a,b,c,*}, Jinlong Ma^{a,b,c}, Weifen Zhang^{a,b,c,*}

^a College of Pharmacy, Weifang Medical University, Weifang 261053, China

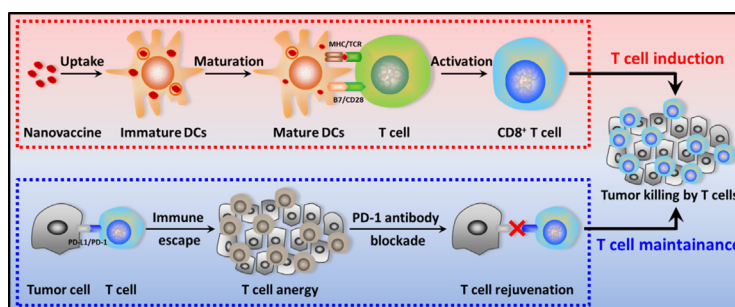
^b Collaborative Innovation Center for Target Drug Delivery System, Weifang Medical University, Weifang 261053, China

^c Shandong Engineering Research Center for Smart Materials and Regenerative Medicine, Weifang Medical University, Weifang 261053, China

HIGHLIGHTS

- Facile antigen/adjuvant co-loaded nanovaccine made by convenient green preparation.
- The immunological activity of the antigen and adjuvant was maximally preserved.
- The minimalist nanovaccine had excellent stability and antitumor immune activation.
- Nanovaccine combined with PD-1 antibody synergistically enhanced therapy outcome.
- Good practicability for expanding clinical translation and personalized therapy.

GRAPHICAL ABSTRACT



ARTICLE INFO

Article history:

Received 27 April 2021

Revised 1 August 2021

Accepted 17 August 2021

Available online 19 August 2021

Keywords:

Cancer immunotherapy

Nanovaccine

Protamine

OVA

CpG

PD-1

ABSTRACT

Introduction: Tumor vaccine has been a research boom for cancer immunotherapy, while its therapeutic outcome is severely depressed by the vulnerable *in vivo* delivery efficiency. Moreover, tumor immune escape is also another intractable issue, which has badly whittled down the therapeutic efficiency.

Objectives: Our study aims to solve the above dilemmas by cooperating minimalist nanovaccine with PD-1 blockade for effective and feasible cancer immunotherapy.

Methods: The minimalist antigen and adjuvant co-delivery nanovaccine was developed by employing natural polycationic protamine (PRT) to carry the electronegative ovalbumin (OVA) antigen and unmethylated Cytosine-phosphorothioate-Guanine (CpG) adjuvant via convenient chemical bench-free "green" preparation without chemical-synthesis and no organic solvent was required, which could preserve the immunological activities of the antigens and adjuvants. On that basis, PD-1 antibody (aPD-1) was utilized to block the tumor immune escape and cooperate with the nanovaccine by maintaining the tumoricidal-activity of the vaccine-induced T cells.

Results: Benefited from the polycationic PRT, the facile PRT/CpG/OVA nanovaccine displayed satisfactory delivery performance, involving enhanced cellular uptake in dendritic cells (DCs), realizable endosomal

Peer review under responsibility of Cairo University.

* Corresponding authors at: College of Pharmacy, Weifang Medical University, Weifang 261053, China.

E-mail addresses: gxw2603@wfmuc.edu.cn (X. Guan), zhangwf@wfmuc.edu.cn (W. Zhang).

<https://doi.org/10.1016/j.jare.2021.08.011>

2090-1232/© 2021 The Authors. Published by Elsevier B.V. on behalf of Cairo University.

This is an open access article under the CC BY-NC-ND license (<http://creativecommons.org/licenses/by-nc-nd/4.0/>).

escape and promoted stimulation for DCs' maturation. These features would be helpful for the antitumor immunotherapeutic efficiency of the nanovaccine. Furthermore, the cooperation of the nanovaccine with aPD-1 synergistically improved the immunotherapy outcome, profiting by the cooperation of the "T cell induction" competency of the nanovaccine and the "T cell maintenance" function of the aPD-1.

Conclusion: This study will provide new concepts for the design and construction of facile nanovaccines, and contribute valuable scientific basis for cancer immunotherapy.

© 2021 The Authors. Published by Elsevier B.V. on behalf of Cairo University. This is an open access article under the CC BY-NC-ND license (<http://creativecommons.org/licenses/by-nc-nd/4.0/>).

Introduction

Cancer immunotherapy has exhibited immense potential and received tremendous attention involving many advanced breakthroughs for cancer treatment in the past several years [1–3]. Among the multifarious immunotherapy modalities, tumor vaccine has been a potential type of active immunotherapy owing to their superiority in specificity [4,5]. By administering tumor antigens into the body, antitumor immune responses will be stimulated and elicited to recognize and attack the tumor cells. To date, extensive research on tumor vaccines has been conducted basing on peptide and protein subunit antigens by virtue of their unique advantages in safety, manufacture and storage [6,7]. However, due to their low immunogenicity and the vulnerable *in vivo* delivery efficiency of these antigens, the aroused antitumor immune responses were usually inferior, and the limited therapeutic outcomes were far from satisfactory for cancer treatment [8,9].

In order to improve the therapeutic efficiency of these tumor vaccines, the introduction of nanomaterials can effectively improve the antigen *in vivo* delivery efficiency, enhance the antigen immunogenicity, and optimize the vaccine treatment program [10,11]. Nanovaccines with specific properties can be designed according to the actual requirements [12,13]. After encapsulated by the nanomaterials, the antigens would be protected from degradation during *in vivo* transportation [14]. Enhanced uptake in antigen-presenting cells (APCs) would be realized by incorporating some cationic or cell-penetrating materials in the nanovaccines [15]. By modification with some specific antibodies or targeting ligands, APC targeting properties would be empowered for the nanovaccines [16]. Besides, controlled or sustained release of the antigens could also be regulated by the nanocarriers in a desired manner [17]. Some membrane-disrupting materials could crack the endosomes and assist the antigen escaping into cytoplasm for contributing to the antigen cross-presentation [18]. Furthermore, antigens and adjuvants could be co-loaded in the nanovaccines, which would increase the immunogenicity and immunostimulatory effect of the nanovaccines to prime powerful antitumor immune responses of the body and improve the cancer immunotherapy efficiency [11,19]. At present, nanovaccine has already been one of the research hotspots in cancer immunotherapy [13,20]. However, many reported nanovaccines usually involved complicated synthesis and modification processes which encompassed various technical and manufactural challenges. Therefore, it is practical to develop nanovaccines possessing characteristics of simple synthesis, affordable manufacture, scalable production and feasible clinical translation.

Protamine (PRT), a naturally occurring highly alkaline cationic polypeptide (4–4.25 kDa) containing 32 amino acids and is rich in arginine, and it mainly exists for DNA condensing in the cell nucleus of the mature sperm of fish [21,22]. PRT sulfate is widely used to improve the half-life of the insulin, and it has been also approved by FDA as an effective heparin antidote [23]. Moreover, PRT has universally recognized as an accessible drug for clinical use with a long history due to its high stability, low immunogenicity and good biological safety [24,25]. At the

same time, PRT can adsorb negatively charged molecules (such as DNA, RNA, protein and peptide) via electrostatic interaction to form complex nanoparticles, which can serve as good drug delivery systems (DDS) [26,27]. Enlightened by the utilization of PRT in DDS, we hypothesize that the polycationic PRT can be exploited as a carrier material to construct a tumor antigen and adjuvant co-loaded nanovaccine to improve the *in vivo* delivery efficiency. On the one hand, PRT has very low immunogenicity and immunostimulatory effect, because it does not contain any aromatic amino acids and lacks a rigid structure [28], so it's a suitable material for antigen and adjuvant delivery. On the other hand, the positive PRT can bind the negatively charged antigen and adjuvant synchronously to form the complex nanovaccine, and the arginine-rich sequence of PRT can also assist to cross the cell membrane of APCs easily for an improved uptake [29]. Moreover, the "proton sponge" effect of PRT will facilitate the endosomal escape of the antigen and promote the cross-presentation for inducing the tumor-cytotoxic CD8⁺ T cells to realize potent antitumor immunotherapy [30].

To validate the availability of our hypothesis on PRT-based nanovaccines, in this work, an antigen and adjuvant co-delivery nanovaccine was developed by utilizing polycationic PRT as the carrier material to adsorb the negatively charged model antigen ovalbumin (OVA) and the adjuvant unmethylated Cytosine-phosphorothioate-Guanine (CpG) via electrostatic interaction. After simple mixing, PRT would bind with the CpG and OVA, these macromolecules would be condensed to form complex nanoparticles, through this convenient method the PRT/CpG/OVA (abbreviated as PCO) nanovaccine was prepared. By subcutaneous (s.c.) administration, the PCO nanovaccines would be injected into the body, and further they would stimulate the body to generate antigen-specific CD8⁺ T cells with high cytotoxic activity, which could effectively identify and kill tumor cells. Considering that the immune escape effect of the tumors can instigate the T cell anergy [31], which would badly inhibit the functionality and tumoricidal capacity of the nanovaccine-induced T cells [32]. The PD-1 antibody (aPD-1) is employed to block the PD-L1/PD-1 interaction between tumors and T cells, for maintaining the antitumor activity of the nanovaccine-induced T cells. The combination of the PCO nanovaccine with aPD-1 treatment, not only can break the bottlenecks involving the low *in vivo* delivery efficiency of nanovaccine and tumor immune escape effect, but also can synergistically enhance the treatment outcome of the antitumor immunotherapy, profiting by the cooperation of the "T cell induction" competency of the nanovaccine to activate the body's antitumor immune responses and the "T cell maintenance" function of the aPD-1 for reducing the tumor immune escape effect (Fig. 1). The preparation, physical-chemical properties and the immunostimulatory capacity of the PCO nanovaccine would be characterized in detail in the study. Further, the *in vivo* combinational antitumor therapeutic effects and the cooperation mechanism would be systematically evaluated. We hope that the explorations in this study can motivate new ideas for the design and construction of facile nanovaccines, and provide an effective and feasible strategy for improving the cancer immunotherapy efficiency.

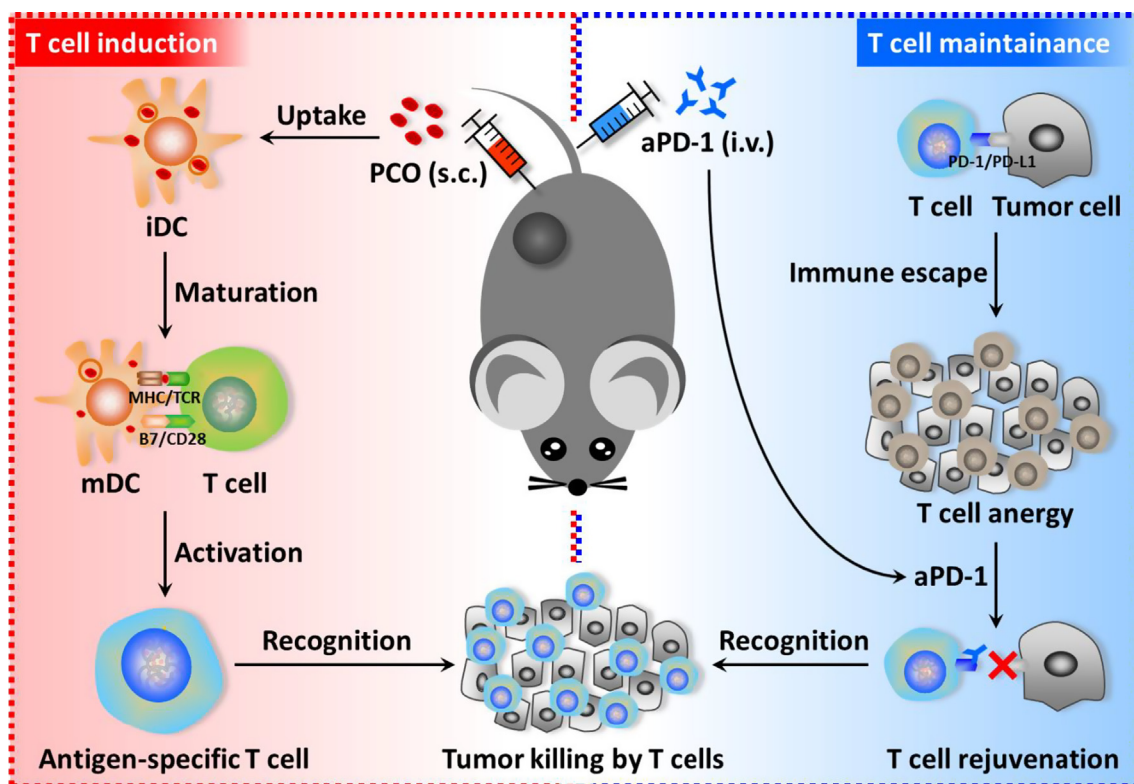


Fig. 1. The cancer immunotherapy strategy by cooperating PCO nanovaccine with aPD-1. PCO nanovaccine was subcutaneously (s.c.) injected into the mice. After uptake the PCO, immature DC (iDC) was stimulated into mature DC (mDC), and further presented the antigen-peptide to T cell for activating antigen-specific T cell. However, tumors could adopt PD-L1/PD-1 pathway to instigate T cell anergy, so aPD-1 was utilized via tail vein injection (i.v.) to block the immune escape and mediate T cell rejuvenation. By cooperating the “T cell induction” of PCO nanovaccine and the “T cell maintenance” of aPD-1, the immunotherapy efficiency would be synergistically enhanced.

Materials and methods

Materials

PRT, OVA, propidium iodide (PI) and lipopolysaccharides (LPS) were purchased from Sigma-Aldrich (St. Louis, MO, USA). CpG 1826 (5'-TCC ATG ACG TTC CTG ACG TT-3') was bought from Sangon (Shanghai, China). Granulocyte-macrophage colony stimulating factor (GM-CSF) and interleukin-4 (IL-4) from mouse were bought from Novus Biologicals (Colorado, USA). The antibodies such as CD11c-PE, CD86-APC, CD80-FITC, CD3e-PE, CD8a-FITC and OVA₂₅₇₋₂₆₄ (SIINFEKL) peptide bound to H-2 K^b APC for flow cytometry (FCM) detection, and the biotinylated OVA₂₅₇₋₂₆₄ (SIINFEKL) peptide bound to H-2 K^b monoclonal antibody for immunofluorescence, these antibodies were all bought from eBioscience (CA, USA). The ELISA kits for mouse interleukin-6 (IL-6), tumor necrosis factor- α (TNF- α) and interferon- γ (IFN- γ) were bought from R&D Systems (Minneapolis, MA, USA). The aPD-1 (InVivoMab anti-mouse PD-1) was purchased from BioXcell (New Hampshire, USA). Avidin-FITC was bought from Boster Bio-Tech (Wuhan, China).

Preparation of the PCO nanovaccine

The PCO nanovaccine was prepared through simple mixing by virtue of the electrostatic interaction between the polycationic PRT and the negatively charged OVA and CpG. Briefly, PRT, CpG and OVA were respectively dissolved in ultrapure water or PBS (pH 7.4, 0.01 M) at the concentrations of 1 mg/mL, 0.5 mg/mL and 1 mg/mL. Different volumes of PRT, CpG and OVA solution were pipetted, and then mixed these three components together

by vortex for 20 s. The mixed solution was further incubated quietly for 30 min to form the complex nanoparticles at room temperature. The component ratio of the PCO nanovaccines could be optionally adjusted to obtain different mass ratios of PCO nanovaccines.

Zeta potential and particle size

The zeta potential, particle size and polydispersity index (PDI) of the PCO nanovaccines were tested by zeta potential/particle size analyzer (Zetasizer Nano ZS90, Malvern Instruments Ltd., UK). The PCO nanovaccines were freshly prepared according to the above mentioned method, and the testing OVA concentration was 25 μ g/mL.

Morphology and stability studies

The morphological feature of the PCO nanovaccine was observed by transmission electron microscope (TEM) with a JEM-1200EX TEM system (NEC, Tokyo, Japan). The PCO nanovaccine aqueous solution was placed onto a 200-mesh carbon-coated copper grid for staying until the samples were completely dried. TEM was operated at 50 kV. The stability of the PCO nanovaccine was monitored by analyzing the particle size fluctuating of the nanovaccines incubated at 37 $^{\circ}$ C in 10% fetal bovine serum (FBS) containing PBS (pH 7.4, 0.01 M) for different times.

Culture of bone marrow-derived dendritic cells (BMDCs)

BMDCs were obtained from the mouse bone marrow cells. C57BL/6 mice (female, 4–6 weeks) were purchased from Vital River

Company (Beijing, China). Before the dissection, the mice were euthanized and further soaked in 75% (v/v) ethanol for sterilization. The femurs and tibias of the hind limbs were obtained for further collecting the bone marrow cells from the bone cavities. The cells were filtered and dispersed by 200-mesh cell strainer. The cells were cultured for 7 days in RPMI 1640 medium with 10% FBS, 100 IU/mL penicillin, 100 mg/mL streptomycin and additive cytokines (including 10 ng/mL GM-CSF and 5 ng/mL IL-4) for stimulating the differentiation of the bone marrow cells to transform into BMDCs.

Cellular uptake in BMDCs

The cellular uptake of the PCO nanovaccines in BMDCs was detected by flow cytometry (FCM). BMDCs were cultured in 6-well plates (1×10^6 cells/well) overnight. The PCO nanovaccines (containing FITC-OVA) were freshly prepared before the experiment. The BMDCs were co-cultured with the PCO nanovaccines (the testing OVA concentration was 5 μ g/mL, containing OVA 10 μ g/well). After 4 h incubation, the BMDCs were collected and washed with PBS. The cellular uptake was detected with a flow cytometer (BD FACS ArianIII, USA).

Cytotoxicity assay in BMDCs

The cytotoxicity of the PCO nanovaccines in BMDCs was tested via PI labeling. The BMDCs were cultured in 6-well plates (1×10^6 cells/well) overnight. The next day, the nanovaccines were prepared and added to the plates (the testing OVA concentration was 5 μ g/mL, containing OVA 10 μ g/well) for incubating with the BMDCs. After 24 h, the BMDCs were gathered and labeled with PI reagent at 4 °C for 30 min. The BMDCs were washed and further detected by FCM (BD FACS ArianIII, USA).

Intracellular localization and endosomal escape

The intracellular localization and the endosomal escape of the PCO nanovaccines in BMDCs were visualized by confocal laser scanning microscopy (CLSM). BMDCs were cultured on sterilized coverslips in 6-well plates (1×10^6 cells/well) overnight. The PCO nanovaccines containing FITC-OVA were freshly prepared and added to the cells (the testing OVA concentration was 5 μ g/mL, containing OVA 10 μ g/well). The BMDCs were incubated with the PCO nanovaccines over different time periods (1 h, 4 h and 6 h). After incubation, the BMDCs were fixed with 4% paraformaldehyde. Cell nuclei were labelled with Hoechst 33,258 for 10 min. The endosomes were stained with Lyso-Tracker Red at 37 °C for 30 min. The result was recorded by CLSM (Leica TCS SP8, Germany).

Maturation of BMDCs

To test the stimulating effect of the PCO nanovaccines on BMDCs maturation, representative co-stimulatory molecules and cytokines were detected. The BMDCs were cultured in 6-well plates (1×10^6 cells/well) overnight. PCO nanovaccines were freshly prepared and added to the cells (the testing OVA concentration was 5 μ g/mL, containing OVA 10 μ g/well). The BMDCs were co-cultured with the PCO nanovaccines. And 24 h later, the culture supernatants and the BMDCs were collected separately. The BMDCs were labeled with CD11c-PE, CD80-FITC and CD86-APC antibodies at 4 °C for 30 min. After that, the BMDCs were washed with PBS and measured by FCM (BD FACS ArianIII, USA). The cytokines including tumor necrosis factor- α (TNF- α) and interleukin-6 (IL-6) in culture supernatants were detected by ELISA kit. The stan-

dard sample was operated to prepare a calibration curve. The OD value of the samples was measured under 450 nm by microplate reader (THERMO FISHER Multiskan FC, USA).

In vivo antitumor therapy

The *in vivo* antitumor therapy was carried out in C57BL/6 mice (female, 6–8 weeks). The B16 melanoma cell line expressing OVA (B16-OVA) was utilized to construct subcutaneous tumor model, the cells were kindly provided by Golden Transfer Science and Technology Co.Ltd. (Changchun, China). The B16-OVA cells were cultivated and expanded to a certain quantity. At day 0, the B16-OVA cells (5×10^5 cells in 100 μ L PBS per mouse) were injected subcutaneously into the back of the mice. These mice were randomly divided into four groups, including PBS, PCO, aPD-1 and PCO + aPD-1. At day 1, the tumor-bearing mice were inoculated with PCO nanovaccines (P/C/O mass ratio = 2/0.5/1, OVA equivalent, 30 μ g/mouse, 100 μ L) via subcutaneous injection, the nanovaccines were weekly administrated for three times. The aPD-1 (40 μ g/mouse, 100 μ L) was administrated into the mice through tail vein injection twice a week for five times. Tumor size and body weight of the mice were regularly recorded during the treatment. The tumor volume was calculated basing the formula: $L \times S^2/2$ (L and S respectively represented the long and short diameter). At the end of the therapy, the mice were euthanized to obtain the tumors and major organs for evaluating the therapeutic effect.

OVA-specific CD8⁺ T cells in tumors

OVA-specific CD8⁺ T cells in tumors were detected by FCM. Fresh tumors were anatomized from the sacrificed mice, the tumors were kept in ice bath and immediately cut into pieces, and the tissues were extruded and dispersed via a 200-mesh cell strainer. The cells were washed with PBS and further labeled with CD3e-PE, CD8a-FITC and OVA₂₅₇₋₂₆₄ (SIINFEKL) peptide bound to H-2 K^b APC antibodies for 30 min. The cells were analyzed by FCM (BD FACS ArianIII, USA).

IFN- γ and TNF- α in tumors

The cytokines including IFN- γ and TNF- α in tumors were measured by ELISA kit. Briefly, the tumor tissues (100 mg) were cut into small pieces and homogenized in cold PBS. After that, the supernatants were gathered through centrifugation and the cytokine contents were evaluated according to the protocols of the ELISA kits. A calibration curve was established with the standard sample. The OD value of the samples was detected under 450 nm by microplate reader (THERMO FISHER Multiskan FC, USA). The concentrations of the samples were further calculated according to the calibration curve.

Histological and immunofluorescence analyses

The biosafety and the levels of the OVA-specific CD8⁺ T cells were respectively evaluated by histological and immunofluorescence analyses. The major organs and the tumors of the sacrificed mice were fixed with 4% paraformaldehyde. These tissues were further embedded in paraffin, and the prepared sections were stained with hematoxylin-eosin (H&E) for histological analysis. The tumor paraffin sections were further processed by immunofluorescence staining for observing OVA-specific CD8⁺ T cells. The biotinylated OVA₂₅₇₋₂₆₄ antibody was utilized for specifically binding the OVA-specific CD8⁺ T cells, and Avidin-FITC was further

added for visualization. The immunofluorescence was recorded by CLSM (Leica TCS SP8, Germany).

Statistical analysis

All measurements were performed in triplicate and presented as mean ± SD. One-way analysis of variance (ANOVA) with Bonferoni’s *post hoc* test was implemented to compare the statistical significance. **p* < 0.05 represented statistically significant. ***p* < 0.01 and ****p* < 0.001 represented extremely significant.

Ethics statement

All experiments involving animals were conducted in accordance with the guidelines for laboratory animals established by the Animal Care and Use Committee of Weifang Medical University (Approval no. 2020SDL101).

Results and discussion

Zeta potential and particle size

The PCO nanovaccines were constructed through a very convenient and time-saving process by simple mixing depending on the electrostatic binding interaction between the polycationic PRT and the negatively charged OVA and CpG. Furthermore, the nanovaccine preparation was a chemical bench-free “green” process without chemical synthesis and modification, and no organic solvent

was required, which could preserve the immunological activities of the antigens and adjuvants. Besides, the modularly constituted PRT/adjuvant/antigen nanovaccine strategy has good flexibility and expandability, other appropriate adjuvants and antigens can also be chosen and loaded in the platform according to the tumor types and characteristics. And the ingredients of the nanovaccines were available and affordable commercialized materials, which were also feasible for clinical translation. Therefore, it was conjectured that the PCO nanovaccine was a simple and practical tumor vaccine construction scenario which would be favored both by researcher and clinician.

To verify the formation of the PCO nanovaccines, the zeta potential and particle size (Fig. 2A and 2B) were detected right after the PCO nanovaccines were prepared freshly. For free CpG/OVA (abbreviated as CO), the zeta potential was −5.61 mV, due to both of the OVA protein and the CpG oligonucleotide were negatively charged innately. The particle size of the CO complex was 855.3 nm, it was speculated that the intertwine effect of the two biomacromolecules might exist to form the relatively unconsolidated particles. After complex with PRT, the CpG and OVA were condensed, and the PCO nanovaccines exhibited a compacted size and held a high positive zeta potential, which confirmed that the polycationic PRT could package the CpG and OVA into nanoparticles effectively. With the PRT ratio increased, the zeta potential was also getting higher, and the particle size of the PCO nanovaccines was slightly undulated, but all of them were below 150 nm, and the PCO nanovaccine with mass ratio of 2/0.5/1 displayed the smallest particle size (117.3 nm). Moreover, it was

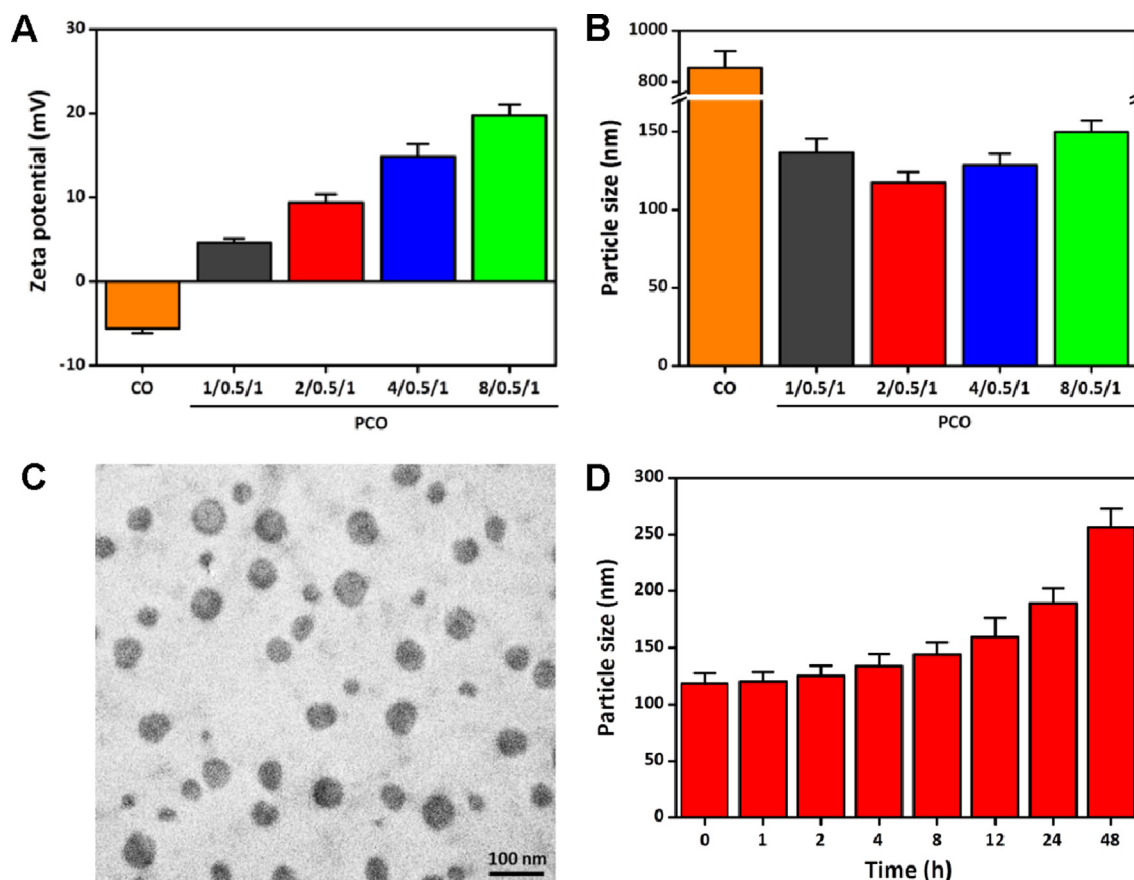


Fig. 2. (A) The zeta potential of the PCO nanovaccines. (B) The particle size of the PCO nanovaccines. For simplicity, the nanoparticles were abbreviated as: CpG/OVA = CO, PRT/CpG/OVA = PCO. (C) The TEM image of the PCO nanovaccines (scale bar = 100 nm). (D) The stability of the PCO nanovaccines incubated in 10% FBS-containing PBS (pH 7.4) for different time.

worth mentioning that the polydispersity index (PDI) of all the PCO nanovaccines was below 0.2 (the data were not shown), which signified a narrow size distribution and relatively homogeneous particle size.

Morphology and stability studies

The morphological feature of the PCO nanovaccines was visualized by TEM. As shown in Fig. 2C and 2D, the PCO nanovaccines exhibited spherical morphology with homogeneous particle size. And the PCO particle size of the TEM result was much smaller than that of the hydrodynamic diameter shown in Fig. 2B, because of the PCO nanoparticles had been shrunken accompanied by water evaporation during the natural drying process. To observe the stability, the PCO nanovaccines were incubated in 10% FBS-containing PBS (simulating physiological environment) for 48 h. As shown in Fig. 2D, the particle size of the PCO nanovaccines changed slightly during the 24 h, which illustrated that the PCO nanovaccines could maintain stable in the body over a sufficient time for APCs capture.

Cellular uptake in BMDCs and cytotoxicity assay

The cellular uptake of nanovaccines by APCs is a prerequisite to stimulate the antigen-specific immune responses. It was reported that the positively charged nanovaccines were apt to access the negatively charged cell membranes via electrostatic attraction, which would facilitate further cellular uptake and internalization of the nanovaccines in APCs [33,34]. Moreover, the nano-sized vaccines also could be captured by the APCs easily [35]. To verify the cellular uptake of the PCO nanovaccines in APCs, BMDCs were generated from the bone marrow cells of the C57BL/6 mice. The cellular uptake of the PCO nanovaccines in BMDCs was detected by FCM. As shown in Fig. 3A, the cellular uptake of the CO group was very low, which meant that the negatively charged unconsolidated CO complexes were not easily phagocytized by BMDCs. However, the PCO nanovaccines presented much higher cellular uptake than CO complexes, which demonstrated that the positive charge and arginine-rich sequence of PRT could assist the PCO nanovaccines to cross the cell membrane of BMDCs and enhance the cellular uptake efficiency significantly. Meanwhile, compared with the CO complexes, the smaller size of the PCO nanovaccines might be another advantage to facilitate the phagocytosis in BMDCs. The result clearly certified that the CpG and OVA co-loaded PCO nanovaccines had efficient cellular uptake in BMDCs.

The cytotoxicity of the PCO nanovaccines against BMDCs was further tested by PI labeling (Fig. 3B). The cell viabilities of the PCO nanovaccines were all above 90%, which were comparable to the PBS group. As a natural polypeptide and FDA approved agent,

PRT owns good biological safety, low immunogenicity and high stability. These unique characteristics of PRT could well meet the requirements of vaccine carrier, therefore it attracted us to explore the feasibility of constructing PRT-based nanovaccines. The cytotoxicity result confirmed that the CpG and OVA co-loaded PCO nanovaccines had no cytotoxicity in BMDCs, which would ensure the DCs exert their functions normally after phagocytizing the PCO nanovaccines.

Intracellular localization and endosomal escape

The intracellular localization and the endosomal escape of the PCO nanovaccines in BMDCs were recorded by CLSM. The BMDCs were incubated with the PCO nanovaccines over different time periods (1 h, 4 h and 6 h). For CLSM observation, FITC-OVA was utilized for nanovaccine preparation and fluorescence tracking. As shown in Fig. 4, after incubation for 1 h, the CO complexes displayed negligible green fluorescence in BMDCs, which meant that tiny amount of CO complexes were internalized in BMDCs. Instead, abundant of green fluorescence appeared in BMDCs for the PCO nanovaccines compared to CO complexes, meaning that a large amount of PCO nanovaccines were rapidly phagocytized and internalized by BMDCs within just one hour, and many of these PCO nanovaccines were found to separate with the endosomes. The result clearly indicated that the polycationic PRT could facilitate the cellular internalization and endosomal escape of the PCO nanovaccines within a short time. After 4 h incubation, the cellular uptake of the CO complexes was still very low, only very little fluorescence signal could be detected in BMDCs. For the PCO nanovaccines, the cellular internalization further increased, the nanovaccines were broadly distributed throughout the whole cytoplasm. Moreover, it could be found from the merged and the enlarged images that the green fluorescence was not co-localized with the red signal, which meant that lots of the PCO nanovaccines had escaped from the endosomes. Further incubation for 6 h, it was inspiring to see that more green fluorescence was disengaged from the red signal, demonstrating that more PCO nanovaccines had broken through the endosome membrane barrier and escaped into the cytoplasm from the endosomes. The “proton sponge” effect of PRT was speculated to play a vital role in disrupting the endosome membrane and assisting the endosomal escape of the antigen. The fled antigens in the cytoplasm would be further processed to accomplish the cross-presentation for priming the antigen-specific CD8⁺ T cells via the major histocompatibility complex class I (MHC I) pathway [36,37]. The CLSM result provided visualized evidence for the efficient cellular internalization and the endosomal escape of the PCO nanovaccines in BMDCs, which would fur-

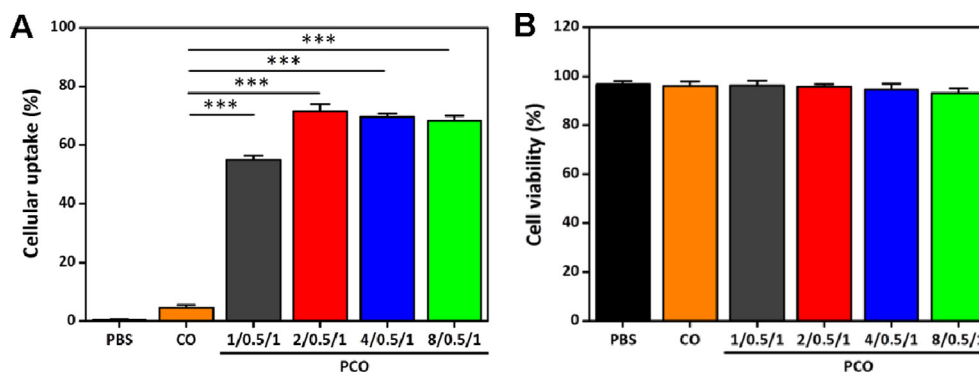


Fig. 3. (A) The cellular uptake of the PCO nanovaccines in BMDCs. FITC-OVA was used for nanovaccine preparation and FCM detection. (B) The cytotoxicity of the PCO nanovaccines against BMDCs for 24 h.

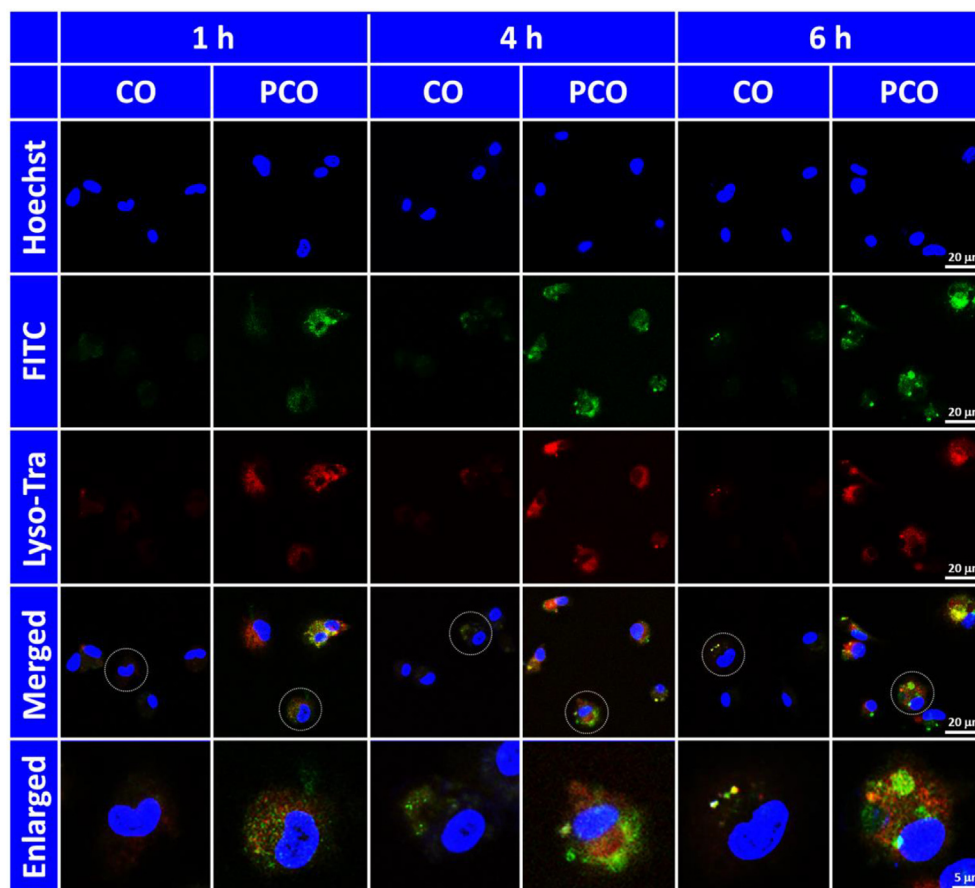


Fig. 4. CLSM images of the BMDCs incubated with the nanovaccines for 1 h, 4 h and 6 h. Cell nucleus was stained blue by Hoechst, FITC-OVA was used for fluorescence tracking, and the endosome was stained red with Lyso-Tracker Red (abbreviated as Lyso-Tra).

ther contribute to induce the maturation of BMDCs and downstream antigen-specific T cell-based immune responses.

Maturation of BMDCs

The maturation of DCs is the key to ensure the antigen presentation for priming the T cells [38,39]. The stimulatory effect of the PCO nanovaccines on BMDC maturation was evaluated by detecting the expression of representative co-stimulatory molecules and the secretion of cytokines. The co-stimulatory molecule CD80 and CD86 on BMDC membrane surface was detected by FCM, and the cytokine IL-6 and TNF- α secretion was measured by ELISA. The results of CD80 and CD86 expression were presented in Fig. 5A-D, and LPS was used as the positive control. The polycationic PRT alone (abbreviated as P) showed slightly lower CD80 and CD86 expression compared with LPS. For CO complexes, the CD80 and CD86 expression was also lower than that of LPS. After loaded by PRT, the PCO nanovaccines exhibited elevated CD80 and CD86 expression, because that the PRT carrying could promote the antigen and adjuvant internalizing into the BMDCs, which would further stimulate the maturation of BMDCs. For the cytokine IL-6 and TNF- α secretion (Fig. 5E and 5F), the PCO nanovaccines also exhibited superlative effect on stimulating the BMDCs to secrete cytokine IL-6 and TNF- α . The above results demonstrated that the PCO nanovaccines had excellent stimulatory effect on BMDC maturation with better improved co-stimulatory molecule expression and cytokine secretion than that of CO complexes.

In vivo antitumor therapy

In order to directly evaluate the performance of the PCO nanovaccines, *in vivo* antitumor therapy was carried out in B16-OVA melanoma model established subcutaneously on C57BL/6 mice. The aPD-1 was employed to enhance the immunotherapeutic efficiency by blocking the immune escape effect of tumors for maintaining the antitumor effects of the nanovaccine-induced T cells. The therapeutic schedule was carefully planned and illustrated in Fig. 6A. At day 0, B16-OVA cells were subcutaneously inoculated into the back of the C57BL/6 mice. Then, the mice were randomly divided into four groups including PBS, PCO, aPD-1 and PCO + aPD-1. At day 1, the tumor-bearing mice were subcutaneously administrated with the PCO nanovaccines weekly for three times. The aPD-1 was further administrated into the mice through tail vein injection twice a week for five times. The tumor size and the body weight of the mice were recorded every three days. After treatment, the mice were euthanized at day 20, the tumors were collected for analyzing the antitumor therapeutic efficiency. As shown in Fig. 6B, the tumor volume rapidly increased for the PBS group, and at day 19, the tumor volume had developed over 2000 mm³, so the therapy was humanely ended considering the laboratory animal welfare and ethics guidelines. The PCO nanovaccine or aPD-1 alone could inhibit the tumor development in a humble manner. Encouragingly, the PCO + aPD-1 group displayed best antitumor therapeutic effect than the other groups, and the growth tendency of the tumor volume was significantly suppressed. In Fig. 6D, the tumors were collected and photographed after the *in vivo* treatment, and it was seen that the tumors of the

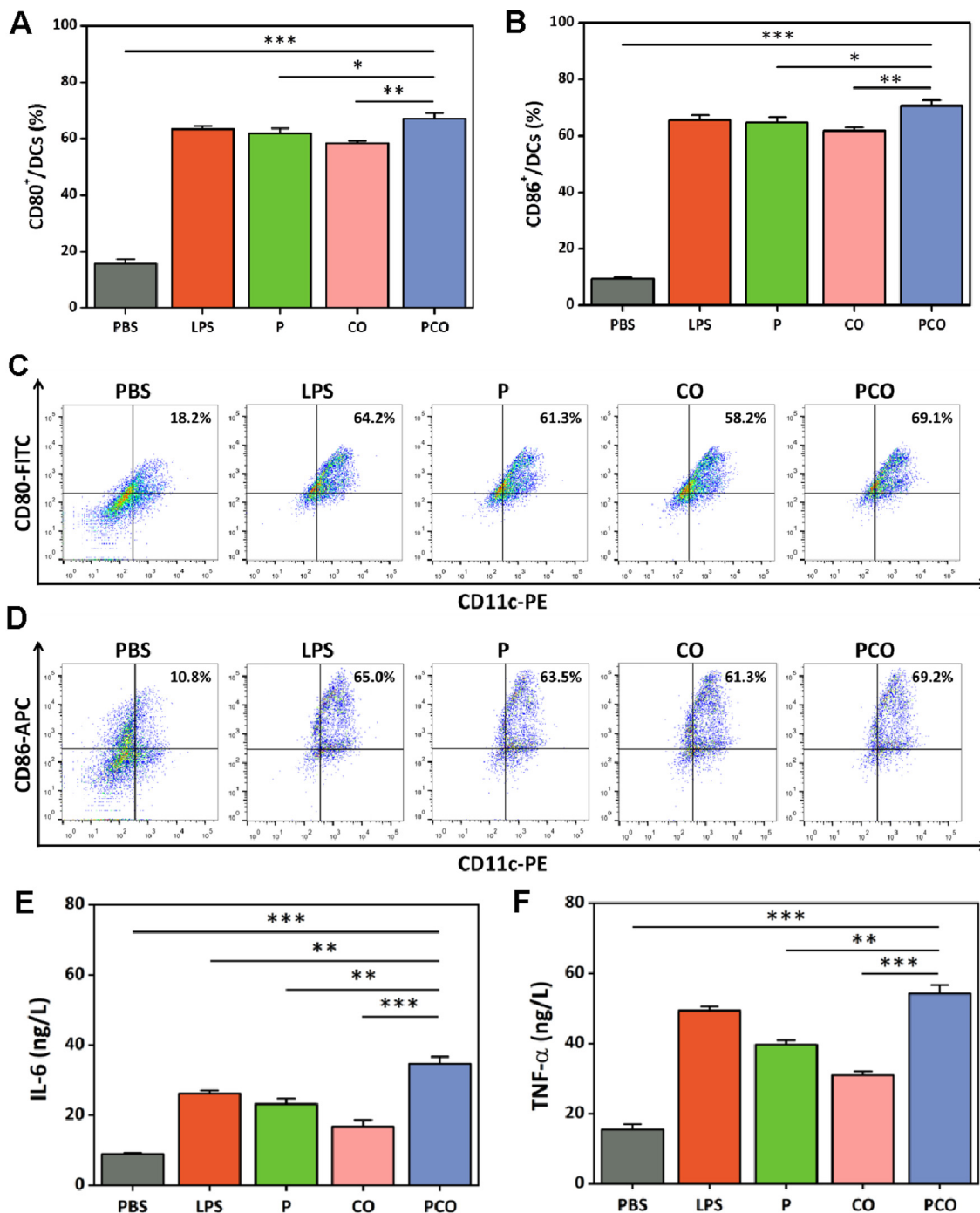


Fig. 5. (A, B) The co-stimulatory molecule CD80 and CD86 expression of the BMDCs incubated with the nanovaccines for 24 h, and (C, D) the corresponding representative FCM plots. (E, F) The cytokine IL-6 and TNF- α secretion in the cell culture supernatants.

PCO + aPD-1 group displayed minimum size compared with the other groups. Furthermore, these tumors were individually weighted one-by-one. As shown in Fig. 6E, the average tumor weight of the PBS, PCO and aPD-1 group was respectively 6.7, 3.6 and 2.6-fold heavier than that of the PCO + aPD-1 group, which indicated that the PCO + aPD-1 group could effectively inhibit the B16-OVA tumor growth. The body weight of the mice was recorded during the treatment, and the result (in Fig. 6C) showed that the body weight of the mice for all the groups revealed a

general trend of steady rise during the first week, and then the body weight of the mice in PBS group increased distinctly with the irrepressible development of the tumors. The PCO group also showed an aberrant weight gain in the last week. By contrast, the aPD-1 and PCO + aPD-1 group displayed slighter increase of body weight than the other two groups, which was mainly due to the effective tumor suppression accompanied with a relatively lighter tumor weight growth. Meanwhile, during the treatment process, no mice died for all the groups, indicating that the PCO

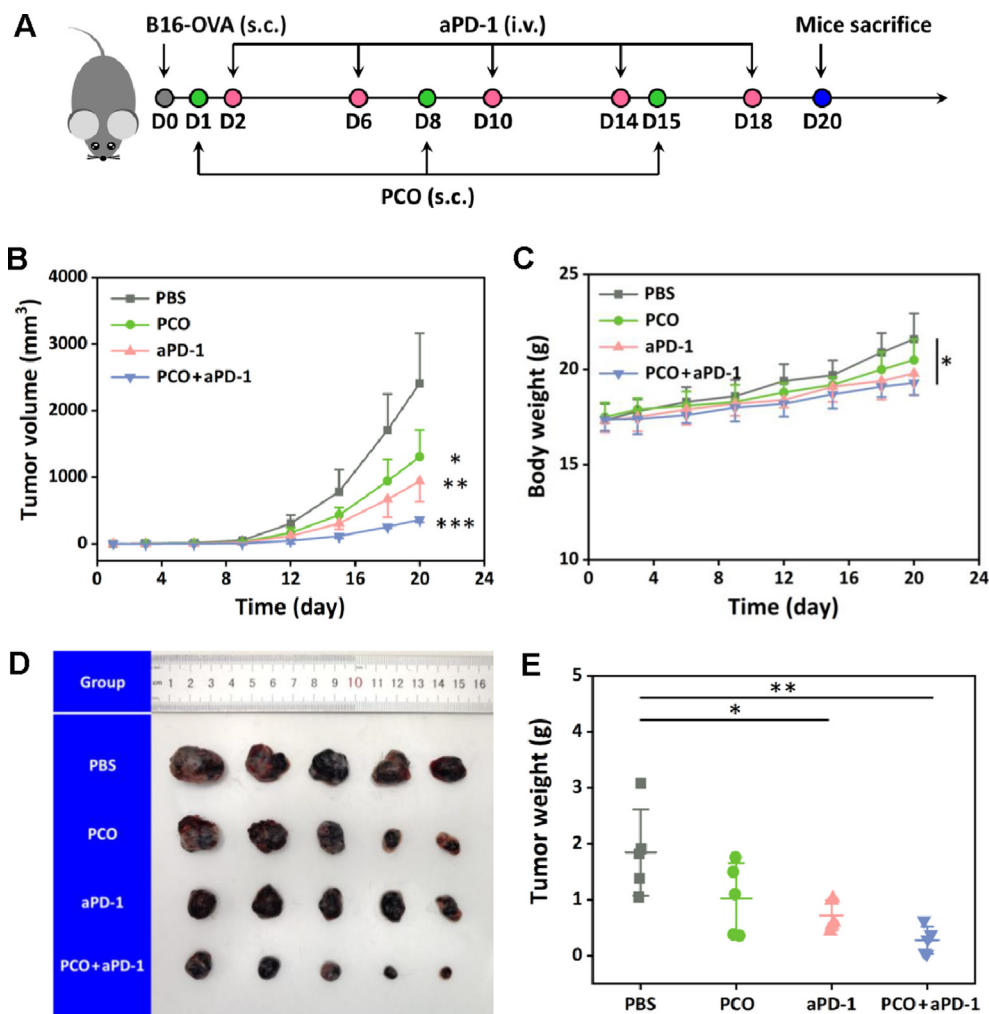


Fig. 6. (A) The therapeutic schedule of the *in vivo* antitumor therapy. (B) Tumor volume of the mice during the treatment. (C) Body weight of the mice during the treatment. (D) Image of the excised tumors after the therapy. (E) Tumor weight of the different groups.

nanovaccine and the aPD-1 administration were safe for the *in vivo* antitumor therapy in mice.

OVA-specific CD8⁺ T cells in tumors

The T cell-based adaptive immunity is crucial in vaccine-induced antitumor immunotherapy [40,41]. To dissect the antitumor effect of the different treatment groups, the T cells and the OVA-specific CD8⁺ T cells in tumors were investigated after the antitumor therapy through FCM. As shown in Fig. 7A and B, the T cell percentage in tumor tissues of the PCO group was higher than that of the PBS group. And more T cells were found to infiltrate in the tumors of the aPD-1 treated mice. More strikingly, the percentage of the T cells in tumors further increased for the PCO + aPD-1 group. The OVA-specific CD8⁺ T cells in tumor tissues were also analyzed, and the result was presented in Fig. 7C and D. Correspondingly, compared with the other groups, the PCO + aPD-1 group displayed the highest percentage of OVA-specific CD8⁺ T cells in tumor tissues. The PCO nanovaccine alone only showed humble effect on T cell infiltration, the immunosuppressive tumor microenvironment might play a negative suppression effect on the PCO nanovaccine-induced T cells. When cooperated with the aPD-1, synergistically enhanced antitumor immune responses of the body were induced by utilizing the aPD-1 to block the tumor

immune escape effect and maintaining the normal antitumor function of the nanovaccine-induced T cells.

IFN- γ and TNF- α in tumors

The cytokine IFN- γ and TNF- α act as crucial effect molecules in the antitumor immunity, and play important roles in the therapeutic outcome [42,43]. Therefore, the production of the INF- γ and TNF- α in the tumors was measured via ELISA. As shown in Fig. 7E, compared with the PBS group, the PCO and aPD-1 group alone could trigger higher content of INF- γ existed in tumors, and the PCO + aPD-1 combination group displayed much superior INF- γ secretion in tumors among the four groups. For the TNF- α (in Fig. 7F), the PCO only slightly increased the TNF- α production. By contrast, the aPD-1 treatment had a better promotion on TNF- α secretion. And consistent with the other results, the PCO + aPD-1 group presented the highest level of TNF- α in tumors than the other groups. The IFN- γ and TNF- α had been reported to play important roles in the modulation of immune responses, and they were crucial cytokines for tumor suppression. The content of IFN- γ and TNF- α in tumor tissues was in coordination with the other results, and all these results indicated that the improved cancer immunotherapy efficiency was achieved by the cooperation of PCO nanovaccine and aPD-1 blockade.

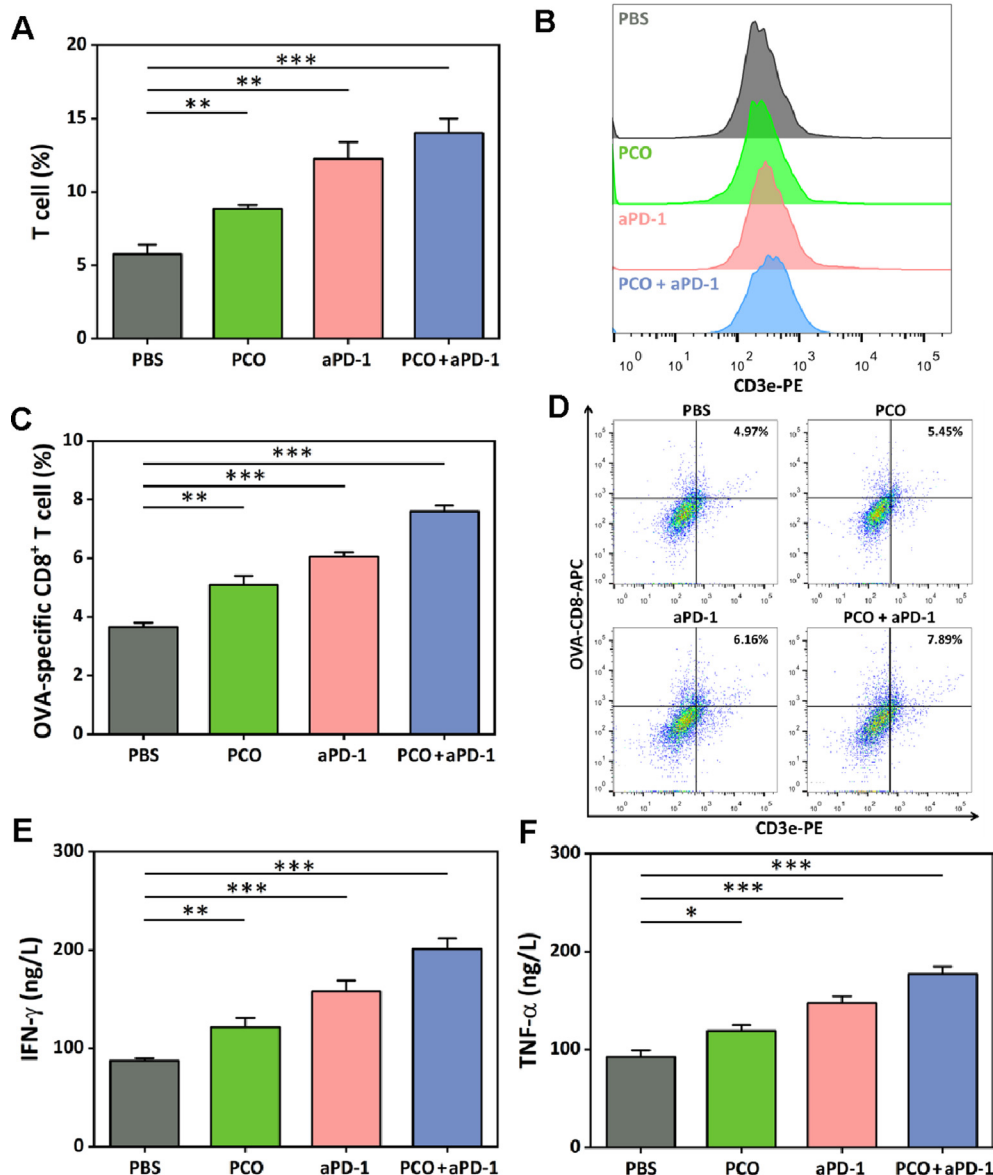


Fig. 7. (A, B) Total T cells in tumors at the end of the antitumor therapy and the representative FCM plot. (C, D) OVA-specific CD8⁺ T cells in tumors and the representative FCM analysis images. (E) The cytokine IFN- γ and (F) TNF- α level in tumors after the treatment.

Histological and immunofluorescence analyses

To assess the histological safety and the antitumor effect of the different treatment groups, H&E staining was implemented by observing the major organs and tumors (Fig. 8A). It could be found that the major organs of all the groups presented normal histological morphology, and the pathological abnormality was not observed in the tissue sections. However, the histological morphology of the tumors treated with different groups had shown some distinctions. For the PBS group, the cell arrangement of the tumors was compact. The PCO or aPD-1 treatment alone had slightly destroyed the tumor tissues. After the PCO + aPD-1 treatment, the tumorous histomorphology had changed dramatically, a large number of tumor cells were destroyed and the cell nuclei were dissolved, displaying the prominent antitumor efficacy of the PCO + aPD-1 combination therapy. The OVA-specific CD8⁺ T cells in tumor tissues were visualized by immunofluorescence staining, and the result was shown in Fig. 8B. Consistent with the FCM result (Fig. 7B), when the tumors were treated with the PCO + aPD-1,

more OVA-specific CD8⁺ T cells were observed in the tumor tissues compared with the other groups. These results collectively demonstrated that the cooperation of PCO nanovaccine with aPD-1 could effectively and feasibly enhance the antitumor immunotherapeutic effect.

Conclusions

In summary, an effective and feasible cancer immunotherapy strategy was proposed in this study by cooperating facile PCO nanovaccine with aPD-1 blockade. This study possesses the following highlights: (1) The minimalist antigen and adjuvant co-delivery nanovaccine was developed with convenient and chemical bench-free “green” preparation process without chemical synthesis and modification, and no organic solvent was required, which could preserve the immunological activities of the antigens and adjuvants. (2) The facile nanovaccine displayed the advantages of easy preparation, good stability and satisfactory antigen-delivery per-

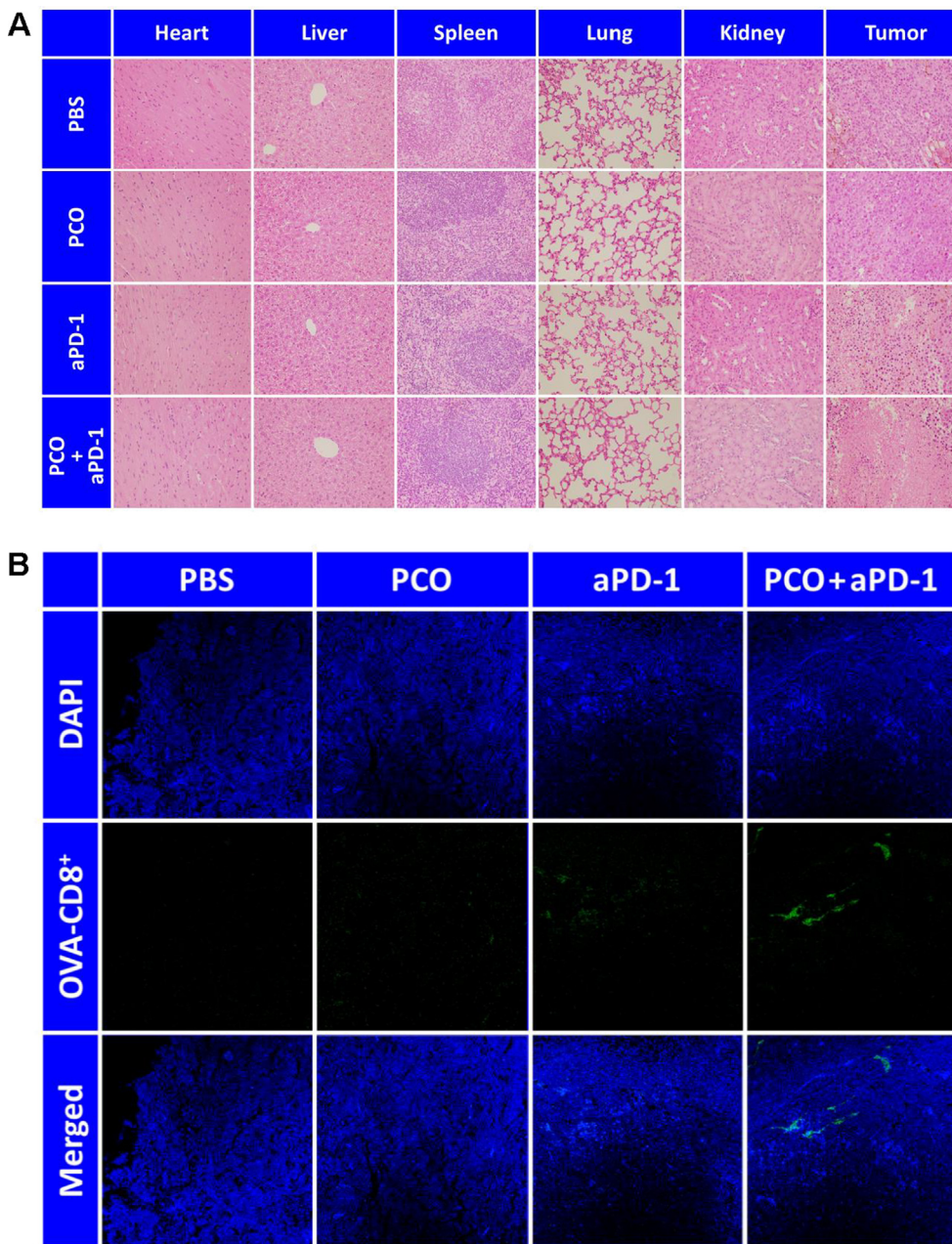


Fig. 8. (A) H&E staining of the major organs and tumors. (B) Immunofluorescence staining of the OVA-specific CD8⁺ T cells in tumors.

formance, involving enhanced cellular uptake in DCs, endosomal escape and promoted stimulation for DC maturation. (3) The combination of the nanovaccine with aPD-1 synergistically enhanced the immunotherapy outcome, profiting by the cooperation of the “T cell induction” competency of the nanovaccine to activate the body’s antitumor immune responses and the “T cell maintenance” function of the aPD-1 for reducing the tumor immune escape effect. By the two-pronged approach, highly enhanced antitumor immunotherapeutic effect was achieved, ensuring the therapeutic scheme more practical and efficient. (4) The modularly constituted PRT/adjuvant/antigen nanovaccine strategy has good flexibility and expandability, other appropriate adjuvants and antigens can also be chosen and loaded in the platform according to the tumor types and characteristics. And the nanovaccine also can be matched with the suitable immune checkpoint antibodies with high response rates, which is conducive to personalized treatment

for specific cases. (5) The ingredients of the nanovaccines were available and affordable commercialized materials. Utilizing the natural polycationic PRT as the carrier not only improved the *in vivo* vaccine delivery efficiency but also expanded the application of the natural PRT material. Furthermore, as a FDA approved safe material for clinical use, PRT is beneficial to the further clinical application and translation. The explorations in this study will motivate new ideas for the design and construction of nanovaccines, and provide important scientific basis for improving the immunotherapy efficiency. Besides, this study also has some limitations. It is important to comprehensively clarify the action mechanism of this nanovaccine, and the safety of the PCO nanovaccine also should be studied systematically. Moreover, the effectiveness of the PCO nanovaccine should be further verified in other tumor models. More detailed and in-depth research will be further conducted in the future. If the basic research can achieve the expected

results, the clinical application and translation are worth looking forward to, and will have great potential in cancer immunotherapy.

Compliance with Ethics Requirements

All Institutional and National Guidelines for the care and use of animals (fisheries) were followed.

Declaration of Competing Interest

The authors declare that they have no known competing financial interests or personal relationships that could have appeared to influence the work reported in this paper.

Acknowledgements

The authors are thankful to the National Natural Science Foundation of China (81973671, 82102883) and the Natural Science Foundation of Shandong Province (ZR2019BEM003) for financial support to this work.

Reference

- Mi Yu, Hagan CT, Vincent BG, Wang AZ. Emerging nano-/microapproaches for cancer immunotherapy. *Adv Sci* 2019;6(6):1801847.
- Andersen MH. Anti-cancer immunotherapy: breakthroughs and future strategies. *Seminars Immunopathol.* 2019;41(1):1–3.
- Riley RS, June CH, Langer R, Mitchell MJ. Delivery technologies for cancer immunotherapy. *Nat Rev Drug Discovery* 2019;18(3):175–96.
- Kroll AV, Jiang Y, Zhou J, Holay M, Fang RH, Zhang L. Biomimetic nanoparticle vaccines for cancer therapy. *Adv Biosyst* 2019;3(1):1800219.
- Tran T, Blanc C, Granier C, Saldmann A, Tanchot C, Tartour E. Therapeutic cancer vaccine: building the future from lessons of the past. *Seminars Immunopathol* 2019;41(1):69–85.
- Tsoras AN, Champion JA. Protein and peptide biomaterials for engineered subunit vaccines and immunotherapeutic applications. *Annual Rev Chem Biomol Eng* 2019;10(1):337–59.
- Foged C. Subunit vaccines of the future: the need for safe, customized and optimized particulate delivery systems. *Therapeutic Delivery* 2011;2(8):1057–77.
- Gause KT, Wheatley AK, Cui J, Yan Y, Kent SJ, Caruso F. Immunological principles guiding the rational design of particles for vaccine delivery. *ACS Nano* 2017;11(1):54–68.
- Zhu G, Zhang F, Ni Q, Niu G, Chen X. Efficient nanovaccine delivery in cancer immunotherapy. *ACS Nano* 2017;11(3):2387–92.
- Liu J, Zhang R, Xu ZP. Nanoparticle-based nanomedicines to promote cancer immunotherapy: Recent advances and future directions. *Small* 2019;15(32):1900262. doi: <https://doi.org/10.1002/smll.v15.3210.1002/smll.201900262>.
- Bhardwaj P, Bhatia E, Sharma S, Ahamad N, Banerjee R. Advancements in prophylactic and therapeutic nanovaccines. *Acta Biomater* 2020;108:1–21.
- Shi K, Haynes MT, Huang L. Nanovaccines for remodeling the suppressive tumor microenvironment: New horizons in cancer immunotherapy. *Front Chem Eng China* 2017;11:676–84.
- Zhang Yu, Lin S, Wang X-Y, Zhu G. Nanovaccines for cancer immunotherapy. *Wiley Interdisciplinary Reviews-nanomedicine and Nanobiotechnology* 2019;11(5). doi: <https://doi.org/10.1002/wnan.v11.510.1002/wnan.1559>.
- Colaprico A, Senesi S, Ferlicca F, Brunelli B, Ugozzoli M, Pallaoro M, et al. Adsorption onto aluminum hydroxide adjuvant protects antigens from degradation. *Vaccine* 2020;38(19):3600–9. doi: <https://doi.org/10.1016/j.vaccine.2020.02.001>.
- Guan X, Chen J, Hu Y, Lin L, Sun P, Tian H, et al. Highly enhanced cancer immunotherapy by combining nanovaccine with hyaluronidase. *Biomaterials* 2018;171:198–206.
- Zhang L, Wu S, Qin Yu, Fan F, Zhang Z, Huang C, et al. Targeted codelivery of an antigen and dual agonists by hybrid nanoparticles for enhanced cancer immunotherapy. *Nano Lett* 2019;19(7):4237–49.
- Cruz IJ, Tacken PJ, Eich C, Rueda F, Torensma R, Figdor CG. Controlled release of antigen and Toll-like receptor ligands from PLGA nanoparticles enhances immunogenicity. *Nanomed Nanotechnol Biol Med* 2017;12(5):491–510.
- Lou J, Zhang Li, Zheng G. Advancing cancer immunotherapies with nanotechnology. *Advanced Therapeutics* 2019;2(4):1800128. doi: <https://doi.org/10.1002/adtp.201800128>.
- Smith DM, Simon JK, Baker Jr JR. Applications of nanotechnology for immunology. *Nat Rev Immunol* 2013;13(8):592–605.
- Sathiyajith CW. Nanovaccines for cancer immunotherapy. *J Vaccines Vaccination* 2017;4(4). doi: <https://doi.org/10.15406/jivv.2017.04.00085>.
- Nematollahi MH, Torkzadehmahanai M, Pardakhty A, Meimand HAE, Asadikaram G. Ternary complex of plasmid DNA with NLS-Mu-Mu protein and cationic liposome for biocompatible and efficient gene delivery: a comparative study with protamine and lipofectamine. *Artif Cells Nanomed Biotechnol* 2017;46:1–11.
- Junghans M, Kreuter J, Zimmer A. Antisense delivery using protamine-oligonucleotide particles. *Nucleic Acids Res* 2000;28:e45.
- Shukla RS, Qin B, Cheng K. Peptides used in the delivery of small noncoding RNA. *Mol Pharm* 2014;11(10):3395–408.
- Alshaer W, Hillaireau H, Vergnaud J, Mura S, Deloménie C, Sauvage F, et al. Aptamer-guided siRNA-loaded nanomedicines for systemic gene silencing in CD-44 expressing murine triple-negative breast cancer model. *J Control Release* 2018;271:98–106.
- Huang Y, Park Y, Moon C, David A, Chung H, Yang V. Synthetic skin-permeable proteins enabling needleless immunization. *Angew Chem* 2010;49(15):2724–7.
- Elzoghby AO, Mostafa SK, Helmy MW, ElDemellawy MA, Sheweita SA. Multi-reservoir phospholipid shell encapsulating protamine nanocapsules for co-delivery of letrozole and celecoxib in breast cancer therapy. *Pharm Res* 2017;34(9):1956–69.
- Vogel V, Lochmann D, Weyermann J, Mayer G, Tziatzios C, van den Broek JA, et al. Oligonucleotide-protamine-albumin nanoparticles: preparation, physical properties, and intracellular distribution. *J Control Release* 2005;103(1):99–111.
- Ando T, Yamasaki M, Protamines SK. Isolation, characterization, structure and function. *Mol Biol Biochem Biophys* 1973;12:1–114.
- Kerkmann M, Lochmann D, Weyermann J, Marschner A, Poeck H, Wagner M, et al. Immunostimulatory properties of CpG-oligonucleotides are enhanced by the use of protamine nanoparticles. *Oligonucleotides* 2006;16(4):313–22.
- Arabzadeh S, Tehranizadeh ZA, Haghighi HM, Charbgo F, Ramezani M, Soltani F. Design, synthesis, and in vitro evaluation of low molecular weight protamine (LMWP)-based amphiphilic conjugates as gene delivery carriers. *Aaps Pharmscitech* 2019;20:111.
- Guan X, Lin L, Chen J, Hu Y, Sun P, Tian H, et al. Efficient PD-L1 gene silencing promoted by hyaluronidase for cancer immunotherapy. *J Control Release* 2019;293:104–12.
- Gao S, Yang D, Fang Y, Lin X, Jin X, Wang Qi, et al. Engineering nanoparticles for targeted remodeling of the tumor microenvironment to improve cancer immunotherapy. *Theranostics* 2019;9(1):126–51.
- Foged C, Brodin B, Frokjaer S, Sundblad A. Particle size and surface charge affect particle uptake by human dendritic cells in an in vitro model. *Int J Pharm* 2005;298(2):315–22.
- Foged C, Arigita C, Sundblad A, Jiskoot W, Storm G, Frokjaer S. Interaction of dendritic cells with antigen-containing liposomes: Effect of bilayer composition. *Vaccine* 2004;22(15-16):1903–13.
- Mottram PL, Leong D, Crimeenirwin B, Gloster S, Xiang SD, Meanger J, et al. Type 1 and 2 immunity following vaccination is influenced by nanoparticle size: Formulation of a model vaccine for respiratory syncytial virus. *Mol Pharm* 2007;4:73–84.
- Chen J, Li Z, Huang H, Yang Y, Ding Q, Mai J, et al. Improved antigen cross-presentation by polyethyleneimine-based nanoparticles. *Int J Nanomed* 2011;6:77–84.
- Wegmann F, Gartlan KH, Harandi AM, Brinckmann SA, Coccia M, Hillson WR, et al. Polyethyleneimine is a potent mucosal adjuvant for viral glycoprotein antigens. *Nat Biotechnol* 2012;30(9):883–8.
- Qian Y, Jin H, Qiao S, Dai Y, Huang C, Lu L, et al. Targeting dendritic cells in lymph node with an antigen peptide-based nanovaccine for cancer immunotherapy. *Biomaterials* 2016;98:171–83.
- Dong Z, Wang Q, Huo M, Zhang N, Li B, Li H, et al. Mannose-modified multi-walled carbon nanotubes as a delivery nanovector optimizing the antigen presentation of dendritic cells. *ChemistryOpen* 2019;8(7):915–21.
- Joyce JA, Fearon DT. T cell exclusion, immune privilege, and the tumor microenvironment. *Science* 2015;348(6230):74–80.
- Zhang J, Endres S, Kobold S. Enhancing tumor T cell infiltration to enable cancer immunotherapy. *Immunotherapy* 2019;11(3):201–13.
- Luo Z, Wu Q, Yang C, Wang H, He T, Wang Y, et al. A powerful CD8⁺ T-cell stimulating D-tetra-peptide hydrogel as a very promising vaccine adjuvant. *Adv Mater* 2017;29(5):1601776. doi: <https://doi.org/10.1002/adma.201601776>.
- Xu J, Wang H, Xu L, Chao Yu, Wang C, Han X, et al. Nanovaccine based on a protein-delivering dendrimer for effective antigen cross-presentation and cancer immunotherapy. *Biomaterials* 2019;207:1–9.